Experimental and Simulation on Enantioselective Extraction in Centrifugal Contactor Separators

Kewen Tang
Dept. of Chemistry and Chemical Engineering, Hunan Institute of Science and Technology, Yueyang 414006, Hunan, China

Dept. of Chemical Engineering, Xiangtan University, Xiangtan 411105, Hunan, China

Hui Zhang
Dept. of Chemical Engineering, Xiangtan University, Xiangtan 411105, Hunan, China

Yongbing Liu
Dept. of Chemistry and Chemical Engineering, Hunan Institute of Science and Technology, Yueyang 414006, Hunan, China

DOI 10.1002/aic.14004
Published online January 14, 2013 in Wiley Online Library (wileyonlinelibrary.com)

The increasing demand for optically pure compounds stimulates the development of new chiral separation processes on an industrial scale. The enantioselective liquid–liquid extraction (ELLE) of phenylsuccinic acid (PSA) enantiomers using hydrophilic hydroxyphenyl-β-CD as extractant (C) was studied experimentally in a countercurrent cascade of 10 centrifugal contactor separators at 293 K. Based on a single-stage equilibrium model and the law of conservation of mass, a multistage equilibrium model of ELLE was developed to investigate the influence of changes in the process parameters such as phase ratios and concentrations on extraction efficiency. The multistage equilibrium model was verified experimentally with a good agreement. The model was applied to predict the symmetrical separation of PSA enantiomers. By modeling, optimal process parameters for the symmetrical separation of PSA enantiomers can be achieved. The minimum number of stages was determined at 22 and 24 for $ee_{eq}>98\%$ and $ee_{eq}>99\%$, respectively.
 AIChE J, 59: 2594–2602, 2013
Keywords: multistage modeling, simulation, extraction, chiral separation, phenylsuccinic acid enantiomers

Introduction

The preparation of optically pure compounds is a major challenge in the pharmaceutical and fine chemical industry.[1] The technologies to access enantiopure compounds, such as crystallization,[2] simulated moving bed chromatography (SMB),[3,4] liquid membrane,[5–7] enantioselective liquid–liquid extraction (ELLE),[8–25] and so on, are developing fast across the world. Classical crystallization is not always applicable due to its low versatility and excessive solid handling. Because of the limited transport rates in membrane technology and the high costs of SMB, ELLE seems the most promising technology, which is cost-effective and easier to scale up to commercial scale. Therefore, it possesses a broad application range.

Since the first report of ELLE was published as early as 1959, many researchers have attempted the separation of optically active compound by chiral solvent extraction in recent years.[8–25] However, most researchers focus on the studies on the extraction equilibrium and the synthesis of new chiral selectors.[8–22] Recently, a few literatures provide fundamental insights about the reaction engineering mechanism by combining experimental investigation and mathematical modeling to predict and optimize the extraction performance.[23–25] Although ample literature is available for single-stage extraction equilibrium, there are only a few studies providing multistage ELLE.[8–25]

Separation of chiral compounds by multistage ELLE has received increasing attention in the last few years.[26–30] As is well known, because the enantioselectivities of the chiral extractants are rather limited, a large number of theoretical stages are required to obtain a higher purity and a higher yield. Separations of some hydrophobic enantiomers by reactive extraction with hydrophilic cyclodextrin derivatives have been investigated in our recent work, and sufficient enantioselectivities were obtained.[25,31,32] Recently, we reported on the kinetics in reactive extraction for chiral separation of some aromatic acid enantiomers, and sufficiently fast kinetics has been obtained, which will be helpful in the design of extraction processes on a large scale.[33,34]

The centrifugal contactor separator is an example of a compact continuous flow device combining fast mixing of two immiscible liquids with fast phase separation in a small volume. Besides the excellent mass-transfer characteristics,

Correspondence concerning this article should be addressed to K. Tang at tangkewen@sina.com.

the high centrifugal forces allow for the separation of liquids with density differences of only 10 kg/m^3. Due to these beneficial properties, the centrifugal contactor separators (CCSs) are suitable for continuous separation of enantiomers using ELLE. The studies on the multistage mathematical model have been rarely reported. Recently, centrifugal contactor separator devices have been applied in continuously ELLE of enantiomers, and an experimental and modeling study has been performed.[35]

For an economically feasible process, it is necessary to know how to optimize process parameters such as the extract phase/washing phase ratio (W/O), the extract phase/feeding phase ratio (W/F), extractant concentration, enantiomer concentration, and the location of feed, to achieve a high yield and product purity in a multistage extractor. A further experimental and modeling study is required to optimize process parameters to realize good yield and good purity at the minimum number of stages.

Here, we report on the use of centrifugal contactor separators for continuous separation of phenylsuccinic acid (PSA) enantiomers by multistage ELLE. A multistage equilibrium model of ELLE was constructed based on the existing single-stage description comprising the chemical and physical equilibrium of the system. The experimental data were modeled using an equilibrium approach.

Experimental

Materials

Hydroxypropyl-β-cyclodextrin (HP-β-CD) was supplied by Qianhui Fine Chemicals (Shangdong, China). PSA (racemate, purity $\geq$99.9) was purchased from Hubei Hongjiang Biochemical (Hubei, China). Solvent for chromatography was of high-performance liquid chromatography (HPLC) grade. All other reagents used in this work were of analytical grade and bought from different suppliers.

Multiextraction experiments

The extract phase (aqueous phase) was prepared by dissolving HP-β-CD in 0.1 mol/L NaH_2PO_4/H_3PO_4 buffer solution, and racemic PSA was dissolved in *n*-octyl alcohol to prepare the feeding phase. Extraction experiment was performed by starting the engines of all CCSs and starting the extract (aqueous phase) pump. After starting the extract pump, the CCSs were filled up in the order from Stage 10 to Stage 1. After the aqueous phase outflow from Stage 1, the wash streams (organic phase) were started. When the wash flow ran from Stage 10, the feed pump was started. As soon as the feed pump started running, samples were taken every 15 min. The concentrations of A_R and A_S in extract outlet were analyzed using HPLC.

Analytical method

The quantification of PSA enantiomers in extract outlet was performed by HPLC using a UV detector (Merck, Hitachi, Japan) at the UV wavelength of 254 nm. The column was Lichrospher C18 (250 $\times$ 4.6 mm^2 i.d., 5 μm) (Hanbon Science & Technology, China). The mobile phase was 0.1 mol/L NaH_2PO_4 aqueous solution (pH=2.5):acetonitrile (80:20) containing 10 mmol/L HP-β-CD at a flow rate of 1.0 mL/min. The pH of the aqueous phase was measured with a pH electrode and a pH meter (Orion, model 720A).

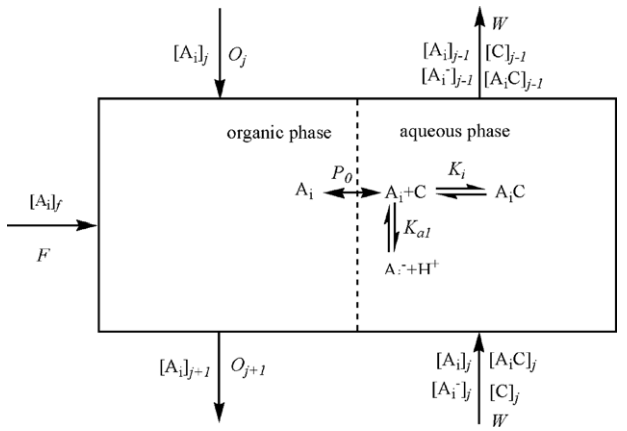

Figure 1. Single extraction stage.

If $j=f$, then $F\neq 0$, else $F=0$, I=R,S.

Theory and Modeling

Extraction mechanism and single extraction equilibrium stage

Knowledge of the extraction mechanism and single-stage equilibrium is important for the optimization of an extraction process. In reactive extraction systems, the reactions may take place in either the organic phase, the aqueous phase or at the interface. In the system for enantioselective extraction of PSA enantiomers with HP-β-CD as extractant, the HP-β-CD is highly hydrophilic, which excludes the possibility that the reaction takes place in the organic phase. Depending on the solubility of PSA enantiomers in the organic phase and the aqueous phase, the location of complexation reaction will either be at the interface or in the aqueous phase. The solutes of PSA enantiomers can distribute over the organic and aqueous phases. Thus, we applied the homogeneous aqueous phase reaction mechanism here (Figure 1).

In our previous studies, the single equilibrium stage model was established by a series of equilibrium relations and mass balance equations, and the model predictions are in good agreement with the experiment.[31] The main parameters in this model involve the chemical properties (complexation constants K_R and K_S, physical partitioning ratio P_0 and acid–base dissociation constant K_{a1}) and the process parameters (temperature, pH, concentrations of extractant [C], and racemic mixture [$A_{R,S}$]). The extent of extraction is characterized by the distribution ratios D_R and D_S for R- and S-PSA

$$D_R=\frac{[A_R]_{aq}^{\text{all form}}}{[A_R]_{org}^{\text{all form}}}=\frac{[A_R]_{aq}+[A_R^-]_{aq}+[A_RC]_{aq}}{[A_R]_{org}} \quad (1)$$

$$D_S=\frac{[A_S]_{aq}^{\text{all form}}}{[A_S]_{org}^{\text{all form}}}=\frac{[A_S]_{aq}+[A_S^-]_{aq}+[A_SC]_{aq}}{[A_S]_{org}} \quad (2)$$

Multistage equilibrium model

A flow scheme of a cascade with N CCSs for the separation of racemic PSA into R- and S-PSA is shown in Figure 2. The organic racemate is fed to the cascade at the feed stage, indicated with f. The stages f to N form the stripping section, where A_R is predominantly extracted to the extract phase (aqueous phase). The coextracted A_S is washed out of the extract stream

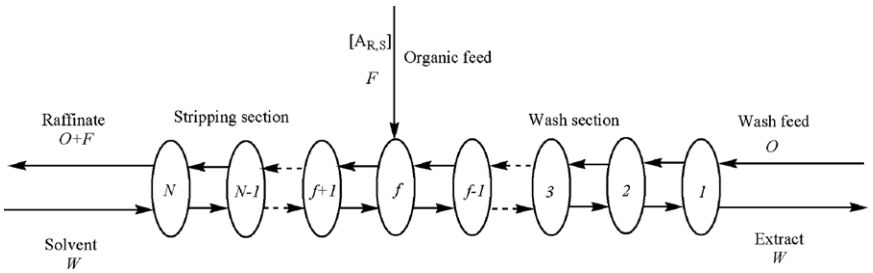

Figure 2. A flow scheme of a cascade with *N* CCSs for separation of PSA enantiomers.

from Stage 1 to $f-1$ (wash section). After multistage extraction, the A_R enantiomer is predominantly left in the extract and the coextracted A_S primarily stays in the raffinate.

A multistage equilibrium model was established based on chemical and physical equilibria. The multistage relations in the cascade follow from Figure 1, in which a single stage from the cascasde is displayed. The solvents are assumed to be completely immiscible, and the extractant C is assumed to be completely insoluble in the organic phase.

For each of the stages ($j=1\ldots N$), the phase equilibrium relations and mass balance equations are shown as follows

The dissociation constant of *R*- and *S*-PSA is defined as

$$K_{a1}=\frac{[H^+]_{aq,j}\left[A_R^-\right]_{aq,j}}{[A_R]_{aq,j}}=\frac{[H^+]_{aq,j}\left[A_S^-\right]_{aq,j}}{[A_S]_{aq,j}} \tag{3}$$

where $[A_R]_{aq}$ and $[A_S]_{aq}$ are the concentrations of the free *R*- and *S*-PSA in aqueous phase at equilibrium, respectively; $\left[A_R^-\right]$ and $\left[A_S^-\right]$ are the concentration of the ionic *R*- and *S*-PSA in aqueous phase at equilibrium, respectively.

The complexation equilibrium constants of *R*- and *S*-PSA with HP-β-CD in aqueous phase are formulated as follows

$$K_R=\frac{[A_RC]_{aq,j}}{[C]_{aq,j}[A_R]_{aq,j}} \tag{4}$$

$$K_S=\frac{[A_SC]_{aq,j}}{[C]_{aq,j}[A_S]_{aq,j}} \tag{5}$$

where $[A_RC]_{aq}$ and $[A_SC]_{aq}$ represent the concentrations of complex *R*-*C* and *S*-*C* in the aqueous phase at equilibrium, respectively; $[C]_{aq}$ is the concentration of free HP-β-CD in the aqueous phase at equilibrium.

The physical partition coefficient of molecular *R*- and *S*-PSA is

$$P_0=\frac{[A_R]_{aq,j}}{[A_R]_{org,j}}=\frac{[A_S]_{aq,j}}{[A_S]_{org,j}} \tag{6}$$

where $[A_R]_{org}$ and $[A_S]_{org}$ are the concentrations of the free *R*- and *S*-PSA, respectively, in organic phase at equilibrium.

For wash section ($j=1\ldots f-1$), the component balances for A_R and A_S are, respectively, defined as

$$W\left([A_R]_{aq,j+1}+\left[A_R^-\right]_{aq,j+1}+[A_RC]_{aq,j+1}\right)+O[A_R]_{org,j-1}=W\left([A_R]_{aq,j}+\left[A_R^-\right]_{aq,j}+[A_RC]_{aq,j}\right)+O[A_R]_{org,j} \tag{7}$$

$$W\left([A_S]_{aq,j+1}+\left[A_S^-\right]_{aq,j+1}+[A_SC]_{aq,j+1}\right)+O[A_S]_{org,j-1}=W\left([A_S]_{aq,j}+\left[A_S^-\right]_{aq,j}+[A_SC]_{aq,j}\right)+O[A_S]_{org,j} \tag{8}$$

If $j=1$, then $[A_R]_{org,\,j-1}=0$ and $[A_S]_{org,\,j-1}=0$

For the feed stage, the component balances for A_R and A_S are respectively defined as

$$F[A_R]_{org,F}+W\left([A_R]_{aq,f+1}+\left[A_R^-\right]_{aq,f+1}+[A_RC]_{aq,f+1}\right)+O[A_R]_{org,f-1}=W\left([A_R]_{aq,f}+\left[A_R^-\right]_{aq,f}+[A_RC]_{aq,f}\right)+(O+F)[A_R]_{org,f} \tag{9}$$

$$F[A_S]_{org,F}+W\left([A_S]_{aq,f+1}+\left[A_S^-\right]_{aq,f+1}+[A_SC]_{aq,f+1}\right)+O[A_S]_{org,f-1}=W\left([A_S]_{aq,f}+\left[A_S^-\right]_{aq,f}+[A_SC]_{aq,f}\right)+(O+F)[A_S]_{org,f} \tag{10}$$

The following equations represent mass balance for A_R and A_S in stripping section ($j=f+1\ldots N$), respectively.

$$W\left([A_R]_{aq,j+1}+\left[A_R^-\right]_{aq,j+1}+[A_RC]_{aq,j+1}\right)+(O+F)[A_R]_{org,j-1}=W\left([A_R]_{aq,j}+\left[A_R^-\right]_{aq,j}+[A_RC]_{aq,j}\right)+(O+F)[A_R]_{org,j} \tag{11}$$

$$W\left([A_S]_{aq,j+1}+\left[A_S^-\right]_{aq,j+1}+[A_SC]_{aq,j+1}\right)+(O+F)[A_S]_{org,j-1}=W\left([A_S]_{aq,j}+\left[A_S^-\right]_{aq,j}+[A_SC]_{aq,j}\right)+(O+F)[A_S]_{org,j} \tag{12}$$

If $j=N$, then $[A_R]_{aq,j+1}=0$, $\left[A_S^-\right]_{aq,j+1}=0$, $[A_RC]_{org,j+1}=0$, $[A_S]_{aq,j+1}=0$, $\left[A_S^-\right]_{aq,j+1}=0$ and $[A_SC]_{org,j+1}=0$.

The overall component mass balances for the enantiomers A_R, A_S, and C are defined as

$$F[A_R]_{org,F}=W\left([A_R]_{aq,N}+\left[A_R^-\right]_{aq,N}+[A_RC]_{aq,N}\right)+O[A_R]_{org,1} \tag{13}$$

$$F[A_S]_{org,F}=W\left([A_S]_{aq,N}+\left[A_S^-\right]_{aq,N}+[A_SC]_{aq,N}\right)+O[A_S]_{org,1} \tag{14}$$

$$[C]_0=\left([C]_{aq,j}+[A_iC]_{aq,j}\right) \tag{15}$$

where $[C]_0$ is the initial concentration of HP-β-CD in aqueous phase.

Combining Eqs. 3–6, Eqs. 1, 2, and 15 are deduced to

$$D_{R,j}=P_0\left(1+K_R[C]_{aq,j}+\frac{K_{a1}}{[H^+]_{aq,j}}\right) \tag{16}$$

$$D_{S,j}=P_0\left(1+K_S[C]_{aq,j}+\frac{K_{a1}}{[H^+]_{aq,j}}\right) \tag{17}$$

$$[C]_{aq,j}=\frac{[C]_0}{1+K_R[A_R]_{aq,j}+K_S[A_S]_{aq,j}} \tag{18}$$

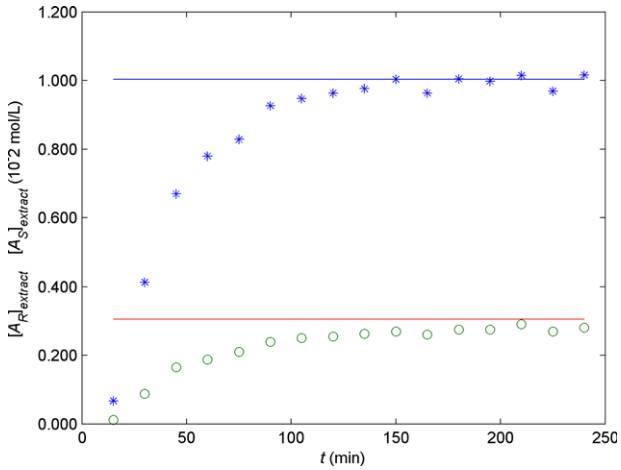

Figure 3. Extraction concentration profiles of the extract exiting.

***W/F*=1.0, *W/O*=3.0, pH=2.5, [$A_{R,S}$]=0.025 mol/L, [*C*]=0.050 mol/L, *f*=6, and *N*=10. Asterisk symbols: experimental data of [A_R], astragal symbols: experimental data of [A_S], dashed line: modeled [A_R], solid line: modeled [A_S]. [Color figure can be viewed in the online issue, which is available at wileyonlinelibrary.com.]**

From Eqs. 16 and 17, the distribution ratios D_R and D_S of each stage are the function of $[H^+]_{aq}$ and $[C]_{aq}$. Equations 7–14 can be simplified by combining Eqs. 16–18.

Enantiomeric excess (*ee*) is used to measure the optical purity of the raffinate and the extract. The definition of *ee* depends on which enantiomer dominates, *ee*>0 (Eq. 19). Note that $[A]_R^{\text{all forms}}$ and $[A]_S^{\text{all forms}}$ encompass A_R and A_S in all forms (free, dissociated, and complexed, so A_R, A_R^-, A_RC, etc.) in this equation.

$$ee = \frac{[A]_R^{\text{all forms}} - [A]_S^{\text{allforms}}}{[A]_R^{\text{allforms}} + [A]_S^{\text{all forms}}} \tag{19}$$

or

$$ee = \frac{[A]_S^{\text{allforms}} - [A]_R^{\text{allforms}}}{[A]_R^{\text{allforms}} + [A]_S^{\text{allforms}}} \tag{20}$$

The yield of the enantiomer *R* in the extract is given in Eq. 21. Similarly, the yield of the enantiomer *S* in the raffinate is defined.

$$\text{yield}_{R,\text{extract}} = \frac{\text{total } A_R \text{ extract}}{\text{total } A_R \text{ feed}} \frac{[\text{mol}]}{[\text{mol}]} \tag{21}$$

The established multistage equilibrium model is based on three assumptions: (1) equilibrium at each stage; (2) a constant temperature at all stages; and (3) a constant pH at all stages. All equilibrium conditions and mass balances on all stages are solved simultaneously. The multistage equilibrium model was programmed in the matlab. By modeling, we investigated the influence of changes in process parameters such as phase ratios, extractant concentration (*C*), and racemate concentration ($A_{R,S}$) on *ee* and yield.

Results and Discussion

Here, the experimental study is reported on separation of PSA enantiomer by ELLE in a countercurrent cascade of 10 centrifugal contactor separators. The 10-stage CCS cascade was run successfully for 6 h at 293 K. The racemic feed entered the cascade at Stage 6. Enantiopure A_R was collected in the extract (aqueous phase), and the raffinate from the cascade contained excess A_S. The concentration in the aqueous outlet was measured every 15 min. Figure 3 depicts the concentrations of the aqueous outlet. The aqueous outlet concentrations increase gradually during the first 2 h. After 2 h steady state was reached. The lines in Figure 3 represent model predictions. The model prediction exhibits a good agreement with the experimental results. The above results suggest that the time needed for physical and chemical equilibrium to establish is very short, and the mass-transfer resistance can be ignored.

To better understand the relationship between process parameters and extraction performance, we investigated the influence of changes in process parameters such as flow ratio

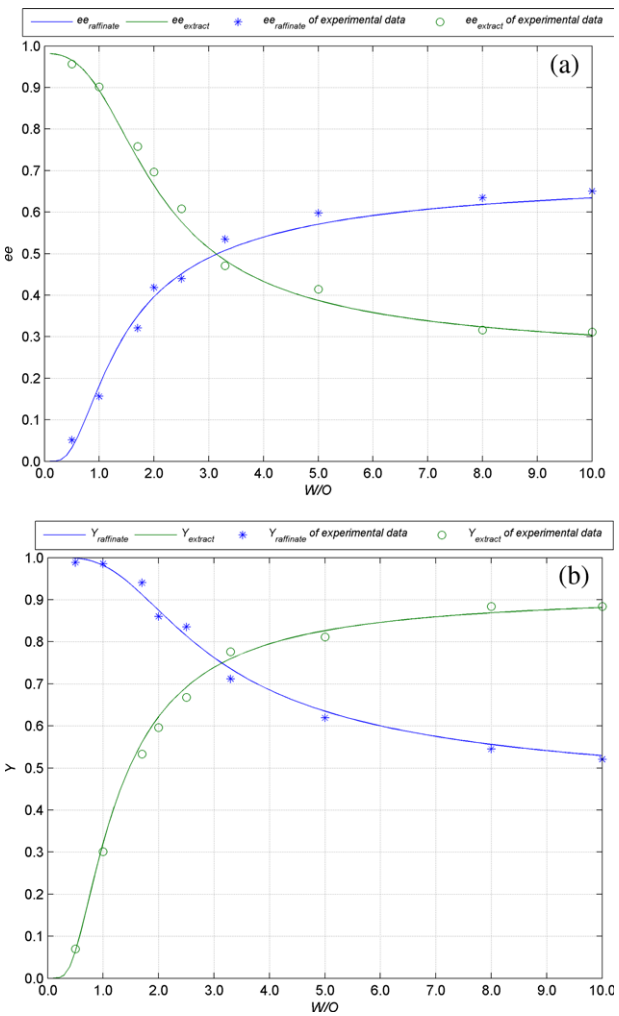

Figure 4. Influence of *W/O* ratio on *ee* and yield for separation of PSA enantiomers.

***W/F*=1.0, pH=2.5, [$A_{R,S}$]=0.025 mol/L, [*C*]=0.050 mol/L, *f*=6, and *N*=10. (a) Influence on *ee* and (b) influence on yield. [Color figure can be viewed in the online issue, which is available at wileyonlinelibrary.com.]**

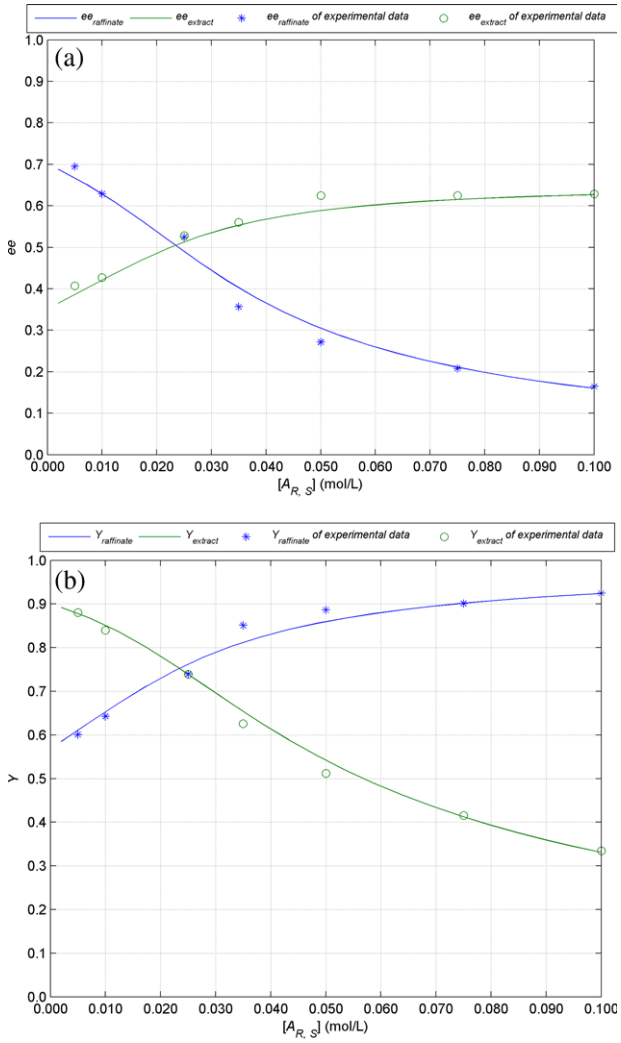

Figure 5. Influence of enantiomer concentration on *ee* and yield for separation of PSA enantiomers.

***W*/*F*=1.0, *W*/*O*=3.0, pH=2.5, [*C*]=0.050 mol/L, *f*=6, and *N*=10. (a) Influence on *ee* And (b) influence on yield. [Color figure can be viewed in the online issue, which is available at wileyonlinelibrary.com.]**

(*W*/*F*, *W*/*O*), enantiomer concentration and extractant concentration on extraction performance by experiment and modeling.

Influence of W/O ratio

The influence of *W*/*O* ratio on purity and yield was investigated in the ratio range of 0.1–10.0 to verify the accuracy of the model (Figure 4). It is indicated from Figure 4 that the model predictions of the *ee* and the yield are in a good agreement with the experimental data.

It can be seen from Figure 4a that at constant settings for other parameters, a higher wash stream (lower *W*/*O* ratio) results in more pure extract stream, but in a less pure raffinate stream. It is shown from Figure 4b that the yield of A_R in extract stream increases with *W*/*O*, but the yield of A_S in wash stream decreases. With the increase of extract stream, more A_RC and A_SC complexes are formed in stripping section, and in wash section more enantiomers are washed back from the extract with the increase of wash stream. It is also found that there is only one crosspoint in which the *ee* in both streams are equal, and the yields are also equal. The crosspoint with ee_{eq} and Y_{eq} is the operating point for symmetric separation.

Influence of enantiomer concentration

In an industrial extractor, it is necessary to operate at higher racemete concentration. In fact, we want to produce not only more enantiomers but also higher purity enantiomers. The influence of enantiomer concentration on the *ee* and the yield was investigated by varying the enantiomer concentration from 0.005 to 0.100 mol/L (Figure 5). It can be found from Figure 5 that with the rise of enantiomer concentration, *ee* in the extract increases, but *ee* in the raffinate decreases. However, the yields in the extract and the raffinate follow an opposite tendency. This could be due to the fact that with the increase of enantiomer concentration, more and more extractant complexes with enantiomers and the extractant will eventually become overloaded.

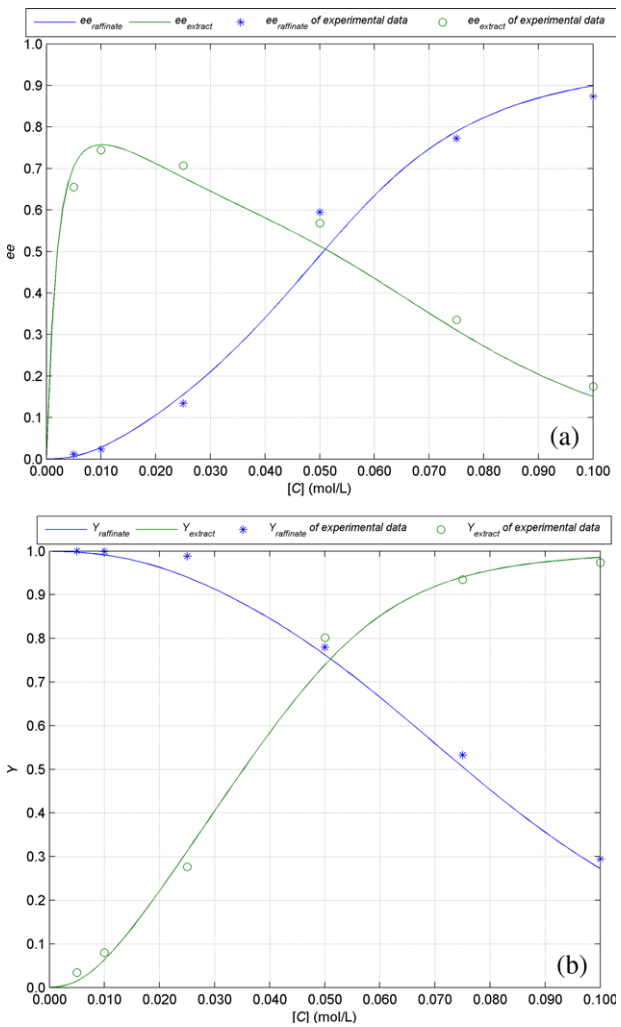

Figure 6. Influence of extractant concentration on *ee* and yield for separation of PSA enantiomers.

***W*/*F*=1.0, *W*/*O*=3.0, pH=2.5, [$A_{R,S}$]=0.025 mol/L, *f*=6, *N*=10. (a) Influence on *ee* and (b) influence on yield. [Color figure can be viewed in the online issue, which is available at wileyonlinelibrary.com.]**

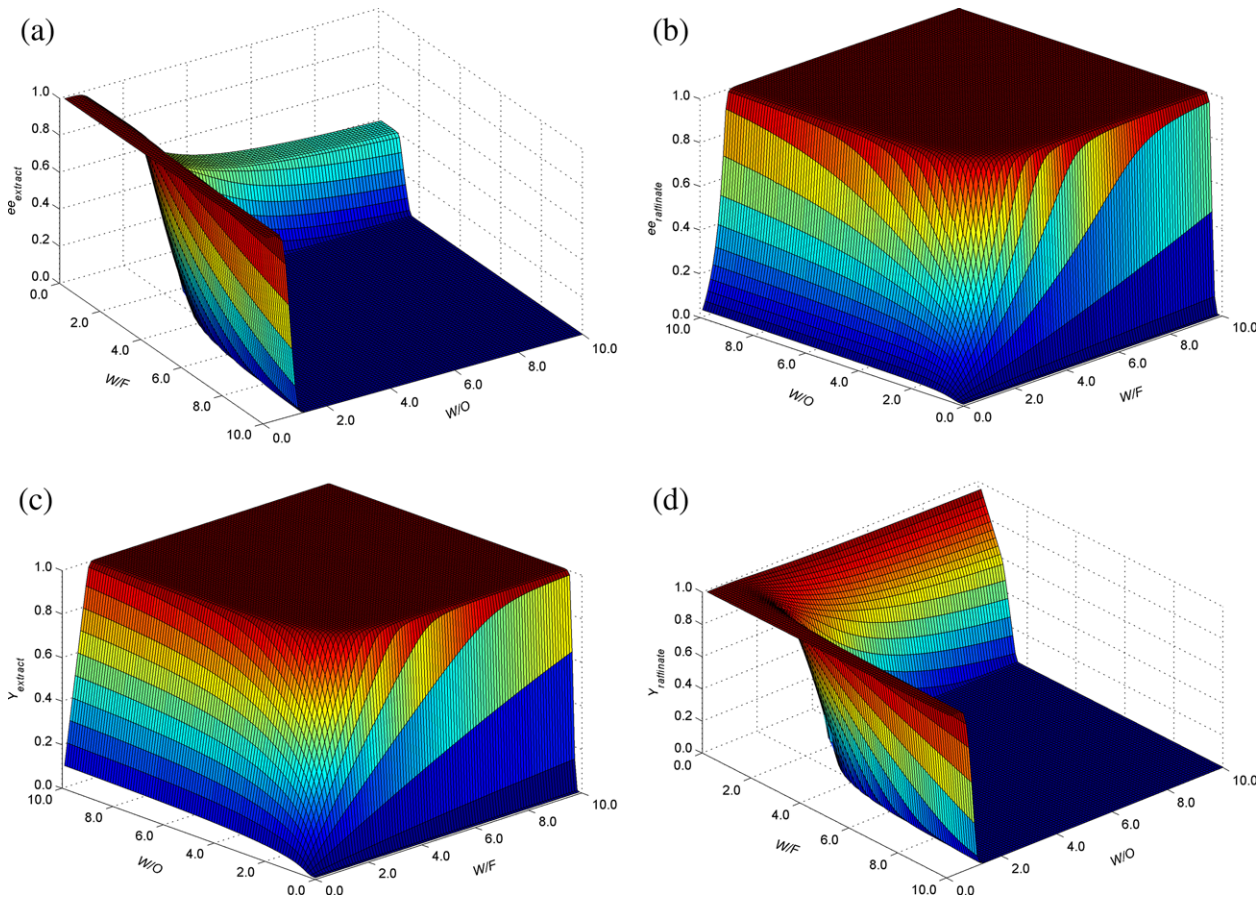

Figure 7. Influence of *W/O* ratio and *W/F* ratio on *ee* and yield for separation of PSA enantiomers.

pH=2.5, [*C*]=0.100 mol/L, [$A_{R,S}$]=0.100 mol/L, feed in middle stage, *N*=24. (a) Influence on *ee* in extract, (b) influence on *ee* in raffinate, (c) influence on yield in extract, and (d) influence on yield in raffinate. [Color figure can be viewed in the online issue, which is available at wileyonlinelibrary.com.]

Influence of extractant concentration

It is necessary to work not only at maximum enantiomers but also at minimal extractant in an industrial production process. The influence of extractant concentration on the purity and yield in both streams was investigated by varying the concentration from 0 to 0.1 mol/L at pH 2.5 and 293 K. A comparison of the experimental data with the model predictions of the purity and yield is shown in Figure 6. A good agreement was obtained between model and experiment.

Figure 6 shows that *ee* in the raffinate and the yield in the extract increase rapidly with the increase of extractant concentration, whereas the yield in the raffinate decreases. A peculiar effect is observed from Figure 6a that the purity in the extract increases with the increase of extractant concentration, reaches a maximum *ee* value, and then decreases with a further increase in extractant concentration.

The fact that the steady-state performance is predicted well by the model, as can be shown in Figures 4–6, further demonstrates that the mass-transfer resistance in the extraction system can be ignored and that the extractor volume is already sufficiently large and can be reduced without performance deterioration.

Model Predictions in the Multistage Extraction System

Experimental results show that CCS equipment is suitable for countercurrently ELLE. Comparison of the model predictions with experimental results indicates that the established multistage equilibrium model is a good means of predicting the extract performance of separation of PSA enantiomers in a countercurrent cascade of centrifugal contactor separators over a range of experimental conditions. Therefore, we utilized the model to explore the influence of various operating conditions on extraction efficiency in a multistage system to predict and optimize the separation process.

Flow ratios

Based on the model, the *ee* and the yield in both the streams are predicted as a function of *W/O* ratio and *W/F* ratio, respectively (Figure 7). It can be observed from Figure 7 that there is a significant effect of *W/F* and *W/O* on *ee* and *Y*. As shown in Figure 7a,b, the *ee* in the extract and the *ee* in the raffinate follow an opposite tendency with the change of *W/F* and *W/O*. The decrease of *W/O* and *W/F* can lead to the increase of the *ee* in the extract and the decrease of the *ee* in the raffinate. The influence of *W/F* and *W/O* on Y_{extract} and $Y_{\text{raffinate}}$ is also contrary to that on ee_{extract} and $ee_{\text{raffinate}}$. It can be seen from Figure 7c,d that the increase of *W/O* and *W/F* can result in the increase of the Y_{extract} in the extract and the decrease of the $Y_{\text{raffinate}}$ in the raffinate. And there is a plateau for each of Figure 7a–d where both the *W/F* ratio and the *W/O* ratio are above 2.0.

In most cases, symmetric separation is needed to obtain both A_R and A_S enantiomers with ee_{eq} and Y_{eq}.

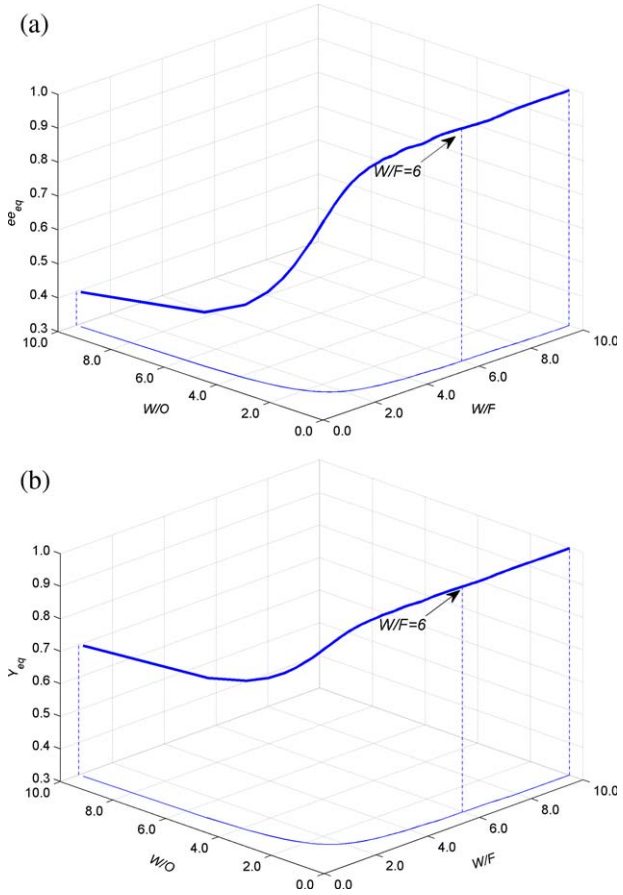

Figure 8. Influence of *W/O* ratio and *W/F* on ee_{eq} and Y_{eq} for separation of PSA enantiomers.

pH=2.5, [*C*]=0.100 mol/L, [$A_{R,S}$]=0.100 mol/L, feed in middle stage, and *N*=24. (a) Influence on ee_{eq} and (b) influence on Y_{eq}. [Color figure can be viewed in the online issue, which is available at wileyonlinelibrary.com.]

The intersecting line of the two surfaces in Figure 7a,b is generated by the two-dimensional interpolation method to explore the influence of *W*/*O* and *W*/*F* on ee_{eq} (Figure 8a). Similarly, the intersecting line of the two surfaces in Figure 7c,d is generated to describe the influence of *W*/*O* and *W*/*F* on Y_{eq} (Figure 8b). As shown in Figure 8, ee_{eq} and Y_{eq} follow a similar tendency with the change of *W*/*F* and *W*/*O*. The ee_{eq} and Y_{eq} increase with the increase of *W*/*F* before *W*/*F* is 6 and then keep nearly unchanged when *W*/*F* continues to increase. However, ee_{eq} and Y_{eq} decrease with the increase of *W*/*O*. On the whole, a larger wash flow and a smaller feed flow are required to reach better ee_{eq} and Y_{eq} in both exit streams. In fact, the *W*/*F* ratio of 6 is suitable for separation of PSA enantiomers by ELLE in a countercurrent cascade of centrifugal contactor separators.

Enantiomer concentration and extractant concentration

Figure 9 shows ee_{eq} and Y_{eq} in both exit streams for separation of PSA enantiomers as a function of enantiomer concentration and extractant concentration. Figure 9a,b demonstrates that equal *ee* and equal yield follow a similar tendency with the change of enantiomer concentration and extractant concentration. With the increase of extractant concentration, ee_{eq} and Y_{eq} increase. However, the increase of enantiomer concentration can lead to the decrease of ee_{eq} and Y_{eq}.

Feed flow and enantiomer concentration

To maximizing the production rate, the influence of feed flow and enantiomer concentration on ee_{eq} and Y_{eq} was investigated. Figure 10 indicates ee_{eq} and Y_{eq} as a function of *F*/*W* ratio and enantiomer concentration under condition that the value multiplying *F* with [$A_{R,S}$], namely $F[A_{R,S}]_F$, is kept constant. It is observed from Figure 10 that the ee_{eq} and Y_{eq} increase with the increase of enantiomer concentration, but decrease with the increase of *F*/*W*. It can be concluded from Figure 10 that, at a constant $F[A_{R,S}]_F$, higher ee_{eq} and Y_{eq} can be obtained at higher $[A_{R,S}]_F$ and lower *F*, which is in accordance with the above results.

For an economically feasible process, $[A_{R,S}]_F$ can be close to the solubility of $A_{R,S}$ ($[A_{R,S}]_{F,S}$) in the feed stream. In a countercurrent cascade of CCSs, a maximum production rate is required. The maximum production rate in a countercurrent cascade of CCSs equals ($[A_{R,S}]_{F,S}$ times the flow limit (F_L). To determine the highest possible production rate, the solubility and the flow limit should be determined, as these two factors determine how much A_R and A_S per unit time can be produced. The solubility of $A_{R,S}$ in the feed solvent can be determined experimentally. The flow limit can be obtained from the optimum *W*/*F* achieved by modeling and

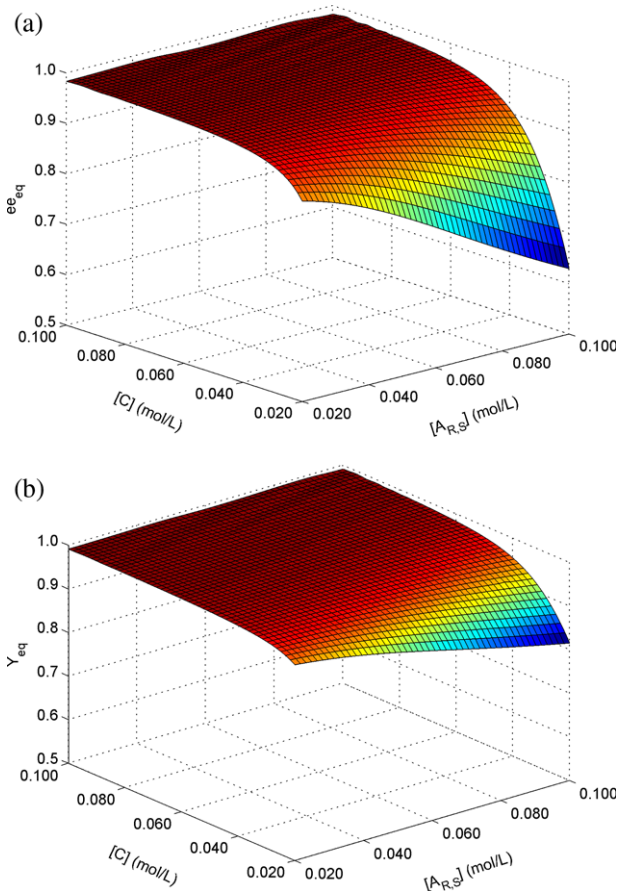

Figure 9. Influence of extractant concentration and enantiomer concentration on ee_{eq} and Y_{eq} for separation of PSA enantiomers.

pH=2.5, *W*/*F*=6.0, *W*/*O*=0.1–10.0, feed in middle stage, *N*=24. (a) Influence on equal *ee* and (b) influence on equal yield. [Color figure can be viewed in the online issue, which is available at wileyonlinelibrary.com.]

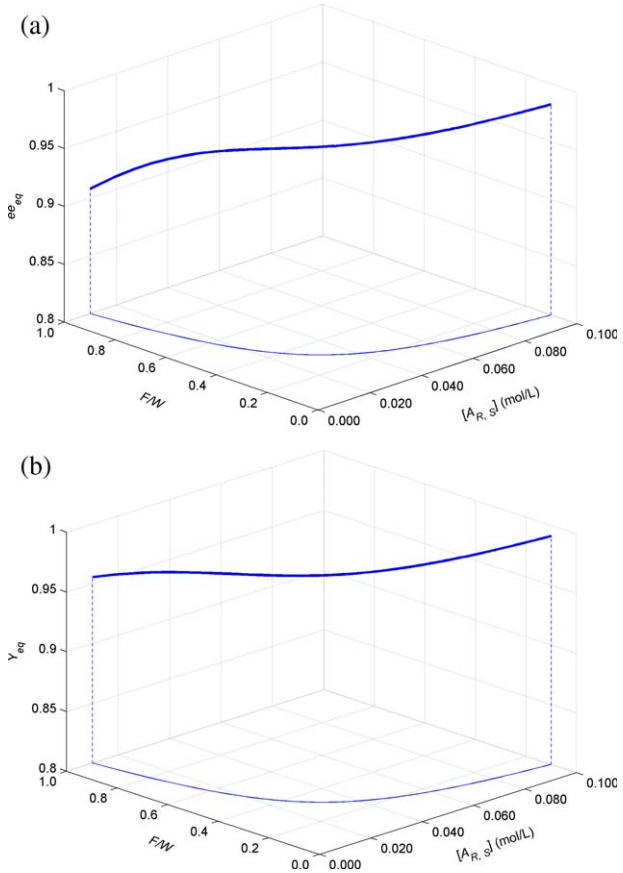

Figure 10. Influence of enantiomer concentration and *F/W* ratio on ee_{eq} and Y_{eq} for separation of PSA enantiomers.

pH=2.5, *W/O*=0.1–10.0, [*C*]=0.100 mol/L, feed in middle stage, *N*=24. (a) Influence on equal *ee* and (b) influence on equal yield. [Color figure can be viewed in the online issue, which is available at wileyonlinelibrary.com.]

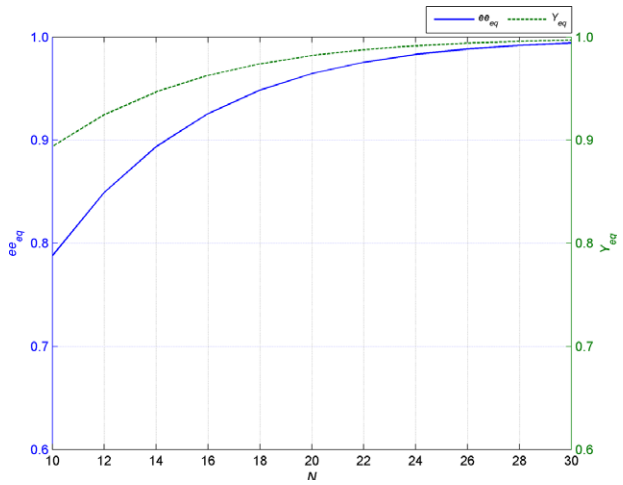

Figure 11. Influence of number of stage on ee_{eq} and Y_{eq} for separation of PSA enantiomers.

***W/F*=6.0, pH=2.5, [*C*]=0.100 mol/L, $[A_{R,S}]$=0.100 mol/L, and feeding in middle stage. [Color figure can be viewed in the online issue, which is available at wileyonlinelibrary.com.]**

Table 1. Optimized Settings for Symmetrical Separations with $[A_{R,S}]$=0.1 mol/L, pH=2.5

Variable	ee_R and ee_S >98% settings	ee_R and ee_S >99% settings
N	22	24
F	12	13
[*C*] (mol/L)	0.1	0.1
W/F	6.0	6.0
W/O	0.6	0.7

the maximum flow rate determined by experiments in a single CCS.[27]

Number of stage

Figure 11 shows ee_{eq} and Y_{eq} as a function of the number of stage from 10 stages to 30 stages by feeding in the middle stage. As shown in Figure 11, ee_{eq} and Y_{eq} increase when the number of stage is less than 20 stages, and there is a plateau where the number of stage is above 20 stages.

For a symmetrical separation, the minimum number of stages was determined for both >99% ee_{eq} and >98% ee_{eq} by modeling. The optimized settings for the two investigated cases are listed in Table 1. When the ee_{eq} should be higher than 98%, a cascade of 22 stages is sufficient, whereas for >99% ee_{eq} a minimum of 24 stages is required. These values are about 1.9 times the predicted values by the Fenske equation for full reflux.[22]

Conclusions and Outlook

It has been demonstrated that the separation of PSA enantiomers $A_{R,S}$ into its enantiomers can be efficiently carried out in CCS equipment by multistage countercurrently enantioselective extraction using hydrophilic hydroxyphenyl-β-CD as extractant. A multistage ELLE model has been developed to investigate the influence of changes in process parameters on extraction efficiency. The model was verified experimentally with excellent results.

The purity and yield can be improved by each measure. The decrease of *W/O* and *W/F* result in the increase of the *ee* in the extract and the decrease of the *ee* in the raffinate. The influence of *W/F* and *W/O* on $Y_{extract}$ and $Y_{raffinate}$ is contrary to that on $ee_{extract}$ and $ee_{raffinate}$. With the increase of extractant concentration, ee_{eq} and Y_{eq} increase, but the increase of enantiomer concentration can lead to the decrease of ee_{eq} and Y_{eq}. Higher ee_{eq} and Y_{eq} can be obtained at higher *W/F*.

The minimum number of stages for complete separation was determined at 22 and 24 for >99% ee_{eq} and >98% ee_{eq} at both exits, respectively, which are 1.9 times larger than the ones predicted by Fenske equation.

Acknowledgments

This work was supported by the Natural Science Foundation of China (No. 21176062), the Open Fund Project of Key Laboratory in Hunan University (No. 11K029), and Aid program for Science and Technology Innovative Research Team in Higher Educational Institutions of Hunan Province.

Notation

C = HP-β-CD (hydroxypropyl-*b*-cyclodextrin), mol/L
P_0 = physical distribution coefficient for PSA

K_{a1} = acid dissociation equilibrium constant, mol/L
D = distribution ratio
K = complexation constants, L/mol
R = R-PSA
S = S-PSA
N = number of stages
ee = enantiomeric excess
Y = yield

Subscripts

i = index for R,S
j = stage index
aq = aqueous phase
org = organic phase
0 = initial value
eq = equal value

Literature Cited

1. Breuer M, Ditrich K, Habicher T, Hauer B, Kesseler M, Sturmerand R, Zelinski T. Industrial methods for the production of optically active intermediates. *Angew Chem Int Ed Engl*. 2004;43:788–824.
2. Gourlay MD, Kendrick J, Leusen FJJ. Predicting the spontaneous chiral resolution by crystallization of a pair of flexible nitroxide radicals. *Cryst Growth Des*. 2008;8:2899–2905.
3. Francotte E, Leutert T, La Vecchia L, Ossola F, Richert P, Schmidt A. Preparative resolution of the enantiomers of *Tert*-leucine derivatives by simulated moving bed chromatography. *Chirality*. 2002;14:313–317.
4. Zenoni G, Quattrini F, Mazzotti M, Fuganti C, Morbidelli M. Scale-up of analytical chromatography to the simulated moving bed separation of the enantiomers of the flavour norterpenoids α-ionone and α-damascone. *Flaour Fragrance J*. 2002;17:195–202.
5. Afonso CAM, Crespo JG. Recent advances in chiral resolution through membrane-based approaches. *Angew Chem Int Ed Engl*. 2004;43:5293–5295.
6. Keurentjes JTF, Nabuurs LJWM, Vegter EA. Liquid membrane technology for the separation of racemic mixtures. *J Membr Sci*. 1996;113:351–360.
7. Maximini A, Chmiel H, Holdik H, Maier NW. Development of a supported liquid membrane process for separating enantiomers of N-protected amino acid derivatives. *J Membr Sci*. 2006;276:221–231.
8. Ohki A, Miyashita R, Naka K, Maeda S. Enantioselective extraction of di-*O*-benzoyltartrate anion by ion-pair extractant having binaphthyl-unit. *Bull Chem Soc Jpn*. 1991;64:2714–2719.
9. Lacour J, Goujon-Ginglinger C, Torche-Haldimann S, Jodry JJ. Efficient enantioselective extraction of tris (diimine) ruthenium(II) complexes by chiral, lipophilic TRISPHAT anions. *Angew Chem Int Ed Engl*. 2000;39:3695–3697.
10. Prelog V, Stojanac Z, Kovacevic K. Separation of enantiomers by partition between liquid-phases. *Hel Chim Acta*. 1982;65:377–384.
11. Tsukube H, Shinoda S, Uenishi J, Kanatani T, Itoh H, Shiode M, Iwachido T, Yonemitsu O. Molecular recognition with lanthanide(III) tris (beta-diketonate) complexes: extraction, transport, and chiral recognition of unprotected amino acids. *Inorg Chem*. 1998;37:1585–1591.
12. Viegas RMC, Afonso CAM, Crespo JG, Coelhoso IM. Modelling of the enantio-selective extraction of propranolol in a biphasic system. *Sep Purif Technol*. 2007;53:224–234.
13. Steensma M, Kuipers NJM, de Haan AB, Kwant G. Influence of process parameters on extraction equilibria for the chiral separation of amines and amino-alcohols with a chiral crown ether. *J Chem Technol Biotechnol*. 2006;81:588–597.
14. Tan B, Luo GS, Wang JD. Extractive separation of amino acid enantiomers with co-extractants of tartaric acid derivative and Aliquat-336. *Sep Purif Technol*. 2007;53:330–336.
15. Jiao FP, Chen XQ, Hu WG, Ning FR, Huang KL. Enantioselective extraction of mandelic acid enantiomers by L-dipentyl tartrate and beta-cyclodextrin as binary chiral selectors. *Chem Pap*. 2007;61(4):326–328.
16. Colera M, Costero AM, Gaviña P, Gil, S. Synthesis of chiral 18-crown-6 ethers containing lipophilic chains and their enantiomeric recognition of chiral ammonium picrates. *Tetrahedron: Asymmetry*. 2005;16:2673–2679.
17. Steensma M, Kuipers NJM, de Haan AB, Kwant G. Identification of enantioselective extractants for chiral separation of amines and aminoalcohols. *Chirality*. 2006;18(5):314–328.
18. Steensma M, Kuipers NJM, de Haan AB, Kwant G. Modelling and experimental evaluation of reaction kinetics in reactive extraction for chiral separation of amines, amino acids and aminoalcohols. *Chem Eng Sci*. 2007;62(5):1395–1407.
19. Dimitrova P, Bart HJ. Extraction of amino acid enantiomers with microemulsions. *Chem Eng Technol*. 2009;32(10):1527–1534.
20. Kocabas E, Karakucuk A, Sirit A, Yilmaz M. Synthesis of new chiral calix[4]arene diamide derivatives for liquid phase extraction of α-amino acid methylesters. *Tetrahedron: Asymmetry*. 2006;17:1514–1520.
21. Verkuijl BJV, Minnaard AJ, de Vries JG, Feringa BL. Chiral separation of underivatized amino acids by reactive extraction with palladium-BINAP complexes. *J Org Chem*. 2009;74(17):6526–6533.
22. Verkuijl BJV, Schuur B, Minnaard AJ, de Vries JG, Feringa BL. Chiral separation of substituted phenylalanine analogues using chiral palladium phosphine complexes with enantioselective liquid–liquid extraction. *Org Biomol Chem*. 2010;8(13):3045–3054.
23. Koska J, Haynes CA. Modelling multiple chemical equilbria in chiral partition systems. *Chem Eng Sci*. 2001;56:5853–5864.
24. Schuur B, Winkelmam JGM, Heeres HJ. Equilibrium studies on enantioselective liquid–liquid amino acid extraction using a cinchona alkaloid extractant. *Ind Eng Chem Res*. 2008;47:10027–10033.
25. Tang KW, Zhang PL, Pan CY, Li HJ. Equilibrium studies on enantioselective extraction of oxybutynin enantiomers by hydrophilic β-cyclodextrin derivatives. *AIChE J*. 2011;57:3027–3036.
26. Steensma M, Kuipers NJM, de Haan AB, Kwant G. Analysis and optimization of enantioselective extraction in a multi-product environment with a multistage equilibrium model. *Chem Eng Proc*. 2007;46:996–1005.
27. Schuur B, Hallett AJ, Heeres HJ, de Vries JG. Scalable enantioseparation of amino acid derivatives using continuous liquid–liquid extraction in a cascade of centrifugal contactor separators. *Org Process Res Dev*. 2009;13:911–914.
28. Abe Y, Shoji T, Fukui S, Sasamoto M, Nishizawa H. Enantioseparation by dual-flow countercurrent extraction: its application to the enantioseparation of (±)-propranolol. *Chem Pharm Bull*. 1996;44:1521–1524.
29. Hallett AJ, Kwant GJ, de Vries JG. Continuous separation of racemic 3,5-dinitrobenzoyl-amino acids in a centrifugal contactor separator with the aid of cinchona-based chiral host compounds. *Chem Eur J*. 2009;15:2111–2120.
30. Schuur B, Floure J, Hallett AJ, Winkelman JGM, de Vries JG, Heeres HJ. Continuous chiral separation of amino acid derivatives by enantioselective liquid–liquid extraction in centrifugal contactor separators. *Org Process Res Dev*. 2008;12(5):950–955.
31. Tang KW, Yi JM, Liu YB, Jiang XY, Pan Y. Enantioselective separation of *R*,*S*-phenylsuccinic acid by biphasic recognition chiral extraction. *Chem Eng Sci*. 2009;64:4081–4088.
32. Tang KW, Song LT, Liu YB, Miao JB. Enantioselective partitioning of 2-phenylpropionic acid enantiomers in a biphasic recognition chiral extraction system. *Chem Eng J*. 2012;180:293–298.
33. Tang KW, Miao JB, Zhou T, Liu YB, Song LT. Reaction kinetics in reactive extraction for chiral separation of α-cyclohexyl-mandelic acid enantiomers with hydroxypropyl-β-cyclodextrin. *Chem Eng Sci*. 2011;66:397–404.
34. Tang KW, Cai J, Zhang PL. Equilibrium and kinetics of reactive extraction of ibuprofen enantiomers from organic solution by HP-β-CD. *Ind Eng Chem Res*. 2012;51:964–971.
35. Schuur B, Winkelman JGM, de Vries JG, Heeres HJ. Experimental and modeling studies on enantio-separation of 3,5-dinitrobenzoyl-(R,S)-leucine by continuous liquid–liquid extraction in a cascade of centrifugal contactor separators. *Chem Eng Sci*. 2010;65:4682–4690.

Manuscript received Jun. 27, 2012, and revision received Dec. 6, 2012.